American Control Conference (ACC), Albuquerque, NM, June 1997.

Optimal Commutation Laws for Torque Control of Synchronous Motors

F. Aghili and M. Buehler
Dept. Mechanical Engineering
McGill University
Montréal, QC H3A 2A7, Canada
{farhad,buehler}@cim.mcgill.ca

J. M. Hollerbach
Dept. Computer Science
University of Utah
Salt Lake City, UT 84112, USA
jmh@cs.utah.edu

Abstract

This paper presents a new model for torque generation of synchronous motors and their control based on Fourier coefficients. Since multi-pole motors give rise to high frequency control signals, the dynamics of the current amplifier are no longer negligible. For this case, we present a new commutation strategy which minimizes the torque ripple and the velocity induced change in the torque transfer function. When the amplifier dynamics are negligible, we present a commutation strategy which delivers ripple-free torque and simultaneously minimizes copper losses. The performance of both commutation laws is validated via simulations based on experimental data from a synchronous motor. The approach can be adapted for general brushless motors.

1. Introduction

Accurate and high bandwidth sources of torque are essential for the precise position, velocity or force control necessary in many robotics and automation applications. Direct drive motors, and in particular synchronous motors [7], are ideal candidates for this task since they eliminate the nonlinear backlash, friction and cogging effects inherent in mechanical transmissions which can severely compromise performance [2].

However, the production of accurate torque is complicated by the nonlinearity of the motor itself. The control problem of how to translate a desired torque command faithfully into a motor torque and the underlying motor model have been studied by several researchers [9, 12, 5, 4, 11, 1]. Manzer [9] characterized variable reluctance motors by approximating their flux linkage through piecewise fits of polynomials. Filicori [5] proposed a torque controller based on a flux observer minimizing copper losses or the maximum motor-feeding voltage. Other approaches are based on transforming currents via the 'd-q transformation' [8]. Since it linearizes only an ideal motor with perfectly sinusoidally distributed magnetomotive force, another torque set point is cascaded to cancel torque ripples [4].

Our first contribution is the formulation of a modelling and control approach where both motor torque function and commutation strategy are expressed by complex truncated Fourier series. We show that the Fourier coefficients of the phase currents and the commutation strategy are related by a set of linear equations. When the amplifier bandwidth is high enough, the solution which yields ripple free torque in general and minimizes copper losses in particular is found by singular value decomposition.

The second contribution is the derivation of a commutation strategy when the amplifier bandwidth is limited. We show that ripple free torque can be accomplished only at one particular velocity. Consequently we propose another commutation law which minimizes the *rms* norm of the torque ripple over a range of selected velocities. We found that the transfer function is a linear time varying system if the amplifier dynamics are linear and show that its variation is minimized by our commutation law. Finally, the delays attributed to the digital controller implementation can be lumped with the transfer function of the current amplifier.

2. System Model

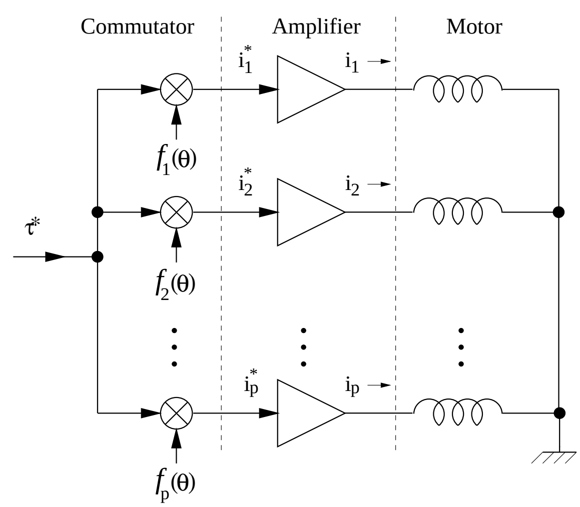

Figure 1: The motor-amplifier-control system.

The structure of the motor torque controller for a general synchronous motor is shown in Fig. 1. The torque generated by a single phase is a function of the phase current, i_r, and the motor angle, θ. In the linear magnetic regime the function is linear in current, and the total torque τ is the sum of the phase torque, τ_r, contributions,

$$\tau(i,\theta) = \sum_{r=1}^{p} \tau_r = \sum_{r=1}^{p} i_r \; g_r(\theta). \tag{1}$$

Since successive phase windings are shifted by $2\pi/p$, we have the following relationship,

$$g_r(\theta) = g(q\theta + 2\pi(r-1)/p),$$

where $g(\theta)$ is the motor's *torque function* and q is the number of motor poles. The commutator commands the phase currents, $i_r^\star$, via

$$i_r^\star(t,\theta) = \tau^\star(t) \; f_r(\theta).$$

The individual phase control signals can be expressed based on the periodic *commutation function* $f(\theta)$,

$$f_r(\theta) = f(q\theta + 2\pi(r-1)/p).$$

Since both $g(\theta)$ and $f(\theta)$ are periodic functions with periodicity of $2\pi/q$, they can be approximated effectively via truncated complex Fourier series,

$$f(\theta) = \sum_{n=-N}^{N} c_n e^{jnq\theta}, \quad g(\theta) = \sum_{m=-N}^{N} d_m e^{jmq\theta}. \tag{2}$$

Since both are real valued functions, their negative Fourier coefficients are the conjugate of their real ones, $c_{-n} = \bar{c}_n$ and $d_{-n} = \bar{d}_n$. As magnetic force is a conservative field, $\oint \tau_r(\theta) d\theta = 0$, implies that $d_0 = 0$. Furthermore, the average of the current waveform should be also zero, and thus $c_0 = 0$. Therefore our motor model, and its control can be completely described by the vectors $C, D \in \mathbb{C}^N$ of Fourier coefficients of $f(\theta)$ and $g(\theta)$ respectively,

$$C = [c_1, c_2, \cdots, c_N]^T, \quad D = [d_1, d_2, \cdots, d_N]^T.$$

The control problem is to find a commutation spectrum vector C when the torque spectrum vector D is given, such that the motor torque τ becomes ripple free, that is, independent of the motor angle θ. With $h(t)$ as the impulse response of the current amplifiers, we have

$$i_r(t) = \int_0^t i_r^\star(\zeta) \; h(t-\zeta) \; d\zeta. \tag{3}$$

After (2) and (3) is substituted into (1) the motor torque can be expressed as

$$\tau(\tau^\star,\theta) = \sum_{r=1}^{p} \left(\sum_{m=-N}^{N} d_m e^{jm(q\theta(t) + 2\pi \frac{r-1}{p})} \right)$$
$$\times \left(\int_0^t \tau^\star(\zeta) \sum_{n=-N}^{N} c_n e^{jn(q\theta(\zeta) + 2\pi \frac{r-1}{p})} \;\; h(t-\zeta) d\zeta \right)$$
$$= \int_0^t \tau^\star(\zeta) \left(\left(\sum_{n=-N}^{N} \sum_{m=-N}^{N} c_n d_m e^{jq(n\theta(\zeta) + m\theta(t))} \right) \right. \tag{4}$$
$$\left. \times \sum_{r=1}^{p} e^{2\pi j \frac{r-1}{p}(n+m)} \right) h(t-\zeta) d\zeta.$$

This expression can be simplified by noting that the third summation term vanishes when $l = m+n$ is not a multiple of the number of phases, p,

$$\sum_{r=1}^{p} e^{2\pi j l \frac{r-1}{p}} = \begin{cases} p & \text{if} \quad l = 0, \pm p, \pm 2p, \pm 3p, \cdots \\ 0 & \text{otherwise.} \end{cases}$$

At constant velocities, $d\theta/dt = \nu$, we have $\theta(t) - \theta(\zeta) = \nu(t-\zeta)$. Defining $\Omega = q\nu$ and $F = pq$, and swapping integration and summation, the torque (4) can be divided into two distinct terms, $\tau(\tau^\star,\theta) = \tau_{rip}(\tau^\star,\theta) + \tau_{lin}(\tau^\star)$, consisting of a position dependent (ripple producing) part

$$\tau_{rip}(\tau^\star,\theta) = p \sum_{\substack{n=-N \\ n\neq 0}}^{N} \sum_{\substack{l=(n-N)/p \\ l\neq n/p}}^{(n+N)/p} c_n d_{pl-n} \; e^{jFl\theta} \tag{5}$$
$$\times \left(\int_0^t \tau^\star(\zeta) e^{-j\Omega n(t-\zeta)} h(t-\zeta) \; d\zeta \right)$$

and a position independent part

$$\tau_{lin}(\tau^\star) = p \sum_{\substack{n=-N \\ n\neq 0}}^{N} \bar{c}_n d_n \int_0^t \tau^\star(\zeta) e^{-j\Omega n(t-\zeta)} h(t-\zeta) \; d\zeta. \tag{6}$$

3. Design of Commutation Laws

3.1. High Amplifier Bandwidth: Minimum Copper Losses

In the absence of significant current amplifier dynamics, the commutation problem has infinitely many solutions. In this case it is possible to minimize the power dissipation

$$P_{loss} = \frac{1}{T} \sum_{r=1}^{p} \int_0^T R \; i_r^2(t) dt$$

where R is the armature resistance. After a change of variable $\theta = \nu t$, the power dissipation can be expressed as

$$P_{loss} = \sum_{j=1}^{P} \frac{R}{2\pi \; q^{-1}} \int_0^{2\pi \; q^{-1}} i_j(\theta)^2 d\theta.$$

By Parseval's theorem [6], we have

$$P_{loss} \propto \sum_{n=-N}^{N} |c_n|^2 = \|C\|_2^2 \tag{7}$$

minimizing power loss is tantamount to minimizing the Euclidean norm of the commutation spectrum vector.

We can ignore the dynamics of the amplifier if its bandwidth is much higher than the frequency of the highest harmonics at maximum velocity, that is $h(t)$ decays faster than $e^{-j\Omega Nt}$. Now $h(t) = \delta(t)$ and the equations (5) and (6) simplify to

$$\begin{aligned} \tau_{lin} &= \tau^\star(pk_0), && (8)\\ \tau_{rip} &= \tau^\star\left(p\sum_{\substack{l=-2N/p\\ l\neq 0}}^{2N/p} k_l\, e^{jFl\theta}\right). && (9)\end{aligned}$$

The term k_0 in (9) is the constant part of the circular convolution of $f(\theta)$ and $g(\theta)$. This, in turn, is equal to the real part of the inner product of the vectors C and D,

$$k_0 = 2\mathcal{R}e < C, D > . \tag{10}$$

The terms k_l are the Fourier coefficients of the ripples which can be calculated as

$$k_l = \begin{cases} \sum_{\substack{n=1\\ n\neq pl}}^{N} c_n d_{pl-n} + \sum_{n=1}^{N-pl} \bar{c}_n d_{n+pl} & \text{if } l < \frac{N}{p} \\ \sum_{n=pl-N}^{pl-1} c_n d_{pl-n} & \text{otherwise.}\end{cases} \tag{11}$$

Now define vector $K = [k_0,\ k_1,\ k_3,\ \cdots,\ k_{2N/p}]^T \in \mathbb{C}^{1+\frac{2N}{p}}$. In order to eliminate the ripple torque (9) completely, all coefficients k_l except k_0 must be zero. Therefore, from (10) and (11) the optimal commutation strategy, C, must solve

$$\begin{array}{l}\mathbf{A}C + \mathbf{B}\overline{C} = pK,\\ \min\|C\|_2.\end{array} \tag{12}$$

where $\mathbf{A}, \mathbf{B} \in \mathbb{C}^{(2\frac{N}{P}+1)\times N}$ can be constructed from the torque spectrum vector D in (9) and (11). For example, for a three phase motor ($p = 3$), matrix B is

$$\mathbf{B} = \begin{bmatrix} d_1 & d_2 & d_3 & d_4 & d_5 & \cdots & d_N\\ d_4 & d_5 & d_6 & d_7 & d_8 & \cdots & 0\\ d_7 & d_8 & d_9 & d_{10} & d_{11} & \cdots & 0\\ \vdots & \vdots & \vdots & \vdots & \vdots & \vdots & \vdots\\ d_{N-2} & 0 & 0 & 0 & 0 & \cdots & 0\\ 0 & 0 & 0 & 0 & 0 & \cdots & 0\\ \vdots & \vdots & \vdots & \vdots & \vdots & \vdots & \vdots\\ 0 & 0 & 0 & 0 & 0 & \cdots & 0\end{bmatrix}$$

and matrix A is given in (13). By separating the real and imaginary parts, (12) can be rewritten in standard linear form

$$\begin{bmatrix} \mathcal{R}e[\mathbf{A}+\mathbf{B}] & -\mathcal{I}m[\mathbf{A}-\mathbf{B}]\\ \mathcal{I}m[\mathbf{A}+\mathbf{B}] & \mathcal{R}e[\mathbf{A}-\mathbf{B}]\end{bmatrix}\begin{bmatrix}\mathcal{R}e\ C\\ \mathcal{I}m\ C\end{bmatrix} = p\begin{bmatrix}\mathcal{R}e\ K\\ \mathcal{I}m\ K\end{bmatrix}. \tag{14}$$

This equation can be expressed concisely as

$$\mathbf{Q}\, X = Y \tag{15}$$

where $\mathbf{Q} \in \mathbb{R}^{(4\frac{N}{p}+2)\times 2N}$, $Y \in \mathbb{R}^{\frac{4N}{p}+2}$, and $X \in \mathbb{R}^{2N}$ is the set of unknown control coefficients. Since all coefficient k_l except k_0 are zero, and $pk_0 = 1$, Y is $Y = [1, 0, 0, \cdots, 0]^T$. In general, for motors with more than two phases, $p > 2$, there are fewer equations than unknowns in (15). Therefore, if Y belongs to the range of Q, a unique solution is not expected. Instead, a family of solutions which belongs to the null space of Q plus a particular solution exist. Among all the solution, the shortest one in the sense of Euclidean norm is desirable. This is consistent with minimizing power losses, since

$$\|C\|_2 = \left\|\begin{bmatrix}\mathcal{R}e\ C\\ \mathcal{I}m\ C\end{bmatrix}\right\|_2.$$

The *pseudo-inverse* is a solution $X_{opt} = \left(\mathbf{Q}^T(\mathbf{Q}\,\mathbf{Q}^T)^{-1}\right)Y$, but has numerical problems in practice because $\mathbf{Q}\mathbf{Q}^T$ may be singular or ill-conditioned. Singular Value Decomposition is a standard technique to deal with such problems [10]. The matrix $\mathbf{Q}$ can be written as $\mathbf{U}\mathbf{\Sigma}\mathbf{V}^T$ where $\mathbf{U}$ and $\mathbf{V}$ are orthogonal matrices and $\mathbf{\Sigma}$ is a diagonal matrix whose elements are the singular values of matrix $\mathbf{Q}$. Since the matrix $\mathbf{Q}$ is not square, it has to be augmented by adding rows of zeros underneath. The inverse of matrix $\mathbf{Q}$ is

$$\mathbf{Q}^{-1} = \mathbf{V}\cdot\left(\mathrm{diag}(\frac{1}{\sigma_i})\right)\cdot\mathbf{U}^T. \tag{16}$$

The inverse of those singular values, σ_i, which are close to zero is replaced by zero. The optimal solution is then $X_{opt} = \mathbf{Q}^{-1}\hat{Y}$, where $\hat{Y}$ is an augmented version of Y. The columns of $\mathbf{V}$ corresponding to the zeroed σ_i construct the bases for the null space of $\mathbf{Q}$ which shows the class of ripple-free commutation law spectrum whereas (16) is the optimum one.

3.2. Limited Amplifier Bandwidth: Minimum Torque Ripples

3.2.1. Torque Transfer Function Before designing the commutation law, it is necessary to derive the system transfer function in the presence of amplifier dynamics. The commutation law aims at eliminating the torque ripple (5), while (6) shows how the current set point $\tau^\star$ is transformed linearly into motor torque. This section is devoted to derive the torque transfer function of the linear system in the presence of amplifier dynamics. Let $\mathcal{G}(t)$ be the impulse function of the system,

$$\tau_{lin}(t) = \mathcal{G}(t)\ * \tau^\star(t).$$

Then by virtue of the convolution integral and (6),

$$\mathcal{G}(t) = 2p\sum_{n=1}^{N}|a_n|\cos(\Omega n t + \angle a_n)h(t), \tag{17}$$

$$
\mathbf{A} = \begin{bmatrix}
\bar{d}_1 & \bar{d}_2 & \bar{d}_3 & \bar{d}_4 & \bar{d}_5 & \bar{d}_6 & \bar{d}_7 & \cdots & \bar{d}_{N-1} & \bar{d}_N \\
d_2 & d_1 & 0 & \bar{d}_1 & \bar{d}_2 & \bar{d}_3 & \bar{d}_4 & \cdots & \bar{d}_{N-4} & \bar{d}_{N-3} \\
d_5 & d_4 & d_3 & d_2 & d_1 & 0 & \bar{d}_1 & \cdots & \bar{d}_{N-7} & \bar{d}_{N-6} \\
\vdots & \vdots & \vdots & \vdots & \vdots & \vdots & \vdots & \vdots & \vdots & \vdots \\
d_{N-1} & d_{N-2} & d_{N-3} & d_{N-4} & d_{N-5} & d_{N-6} & d_{N-7} & \cdots & d_1 & 0 \\
0 & 0 & d_N & d_{N-1} & d_{N-2} & d_{N-3} & d_{N-4} & \cdots & d_4 & d_3 \\
\vdots & \vdots & \vdots & \vdots & \vdots & \vdots & \vdots & \vdots & \vdots & \vdots \\
0 & 0 & 0 & 0 & 0 & 0 & 0 & \cdots & 0 & d_N
\end{bmatrix} \tag{13}
$$

where $a_n = c_n \bar{d}_n$. Thus the impulse response of the torque, $\mathcal{G}(t)$ is formed by modulating $\cos(\Omega nt + \sigma_n)$, the *carrier*, by the amplifier's impulse response, $h(t)$. Modulating a signal by cosine with spectrum $H(j\omega)$ causes replicas of $H(j\omega)$ to be placed at plus and minus the carrier frequency ω. The Fourier transform of the system in terms of the amplifier's frequency response $H(j\omega)$ is

$$
G(j\omega) = p \sum_{n=1}^{N} a_n H(j(\omega + \Omega n)) + \bar{a}_n H(j(\omega - \Omega n)). \tag{18}
$$

The system transfer function depends on the velocity, Ω, such that at zero velocity it is coincident with that of the current amplifiers, $H(j\omega)$. Define $\Delta(j\omega) = G(j\omega) - H(j\omega)$, which is an indication of additive uncertainty when the current amplifier's response is taken as the nominal transfer function of the torque system. The natural question then would be what the maximum velocity induced uncertainty is. Using the Taylor expansion of the shifted functions around ω and ignoring the second and higher order terms, one can write,

$$
|\Delta(j\omega)| \simeq 2\Omega \left| \sum_{n=1}^{N} n \mathcal{I}m \; a_n \right| \cdot |H'(j\omega)|.
$$

This expression relates the uncertainty of the system to $|H'(j\omega)|$. One can show that for first order or damped second order amplifier dynamics, $|H'(j\omega)|$ is maximum at $\omega = 0$, which implies that Ω, $\sup_\omega |\Delta(j\omega)| \simeq |\Delta(j0)|$. The outcome of this part will be used to design the optimal commutator.

3.2.2. Ripple Cancellation Equation (5) is the ripple in the presence of amplifier dynamics. The integral terms indicate that the current still enters linearly. Suppose $\gamma_n(t) = h(t)e^{jn\Omega t}$ is the impulse response of a virtual system associated with the nth harmonics,

$$
\int_0^t \tau^\star(\zeta) e^{jn\Omega(t-\zeta)} \; h(t-\zeta) d\zeta = \gamma_n(t) * \tau^\star(t),
$$

where $*$ denotes the convolution operator. The exponential function shifts the frequency of the Fourier transform of the current amplifier, $H(j\omega)$. Therefore in the frequency domain we have, $\Gamma_n(j\omega) = H(j(\omega + \Omega n))$. The steady-state response of the system to a unit step input is

$$
\lim_{\omega \to 0} \Gamma_n(j\omega) = H(j\Omega n). \tag{19}
$$

Therefore, substituting (19) into (5) yields the steady-state torque ripple. Moreover, since γ_n is a real valued function, $H(-j\Omega n) = \overline{H(j\Omega n)}$. Now the spectrum of the steady-state ripple can be found analogous to the previous case at each particular velocity $\Omega^{(i)} = q\nu^{(i)}$ as

$$
\mathbf{A}\mathcal{H}^{(i)} C + \mathbf{B}\bar{\mathcal{H}}^{(i)} \bar{C} = pK, \tag{20}
$$

where $\mathcal{H}^{(i)} \in \mathbb{C}^{N \times N}$ is a diagonal matrix as

$$
\mathcal{H}^{(i)} = \mathrm{diag}[H(j\Omega^{(i)}\,,\; H(j2\Omega^{(i)})\,,\; \cdots\,,\; H(jN\Omega^{(i)})].
$$

Equation (20) is similar to (12) by substituting $\mathbf{A}\mathcal{H}$ and $\mathbf{B}\bar{\mathcal{H}}$ as $\mathbf{A}$ and $\mathbf{B}$ respectively. Analogous to (15), we have $\mathbf{Q}^{(i)} X = Y$. As a matter of fact, one can show that (15) is the special case where the velocity is set to zero. Therefore, it can be concluded that the minimizing losses commutation law is always applicable at every particular velocity. Such a commutation is useful for velocity regulator applications where the velocity is around an operating point. Since the matrix $\mathbf{Q}^{(i)}$ changes with velocity, we can write the equations over an arbitrary numbers of velocities,

$$
\underbrace{\begin{bmatrix} \mathbf{Q}^{(0)} \\ \mathbf{Q}^{(1)} \\ \mathbf{Q}^{(2)} \\ \vdots \\ \mathbf{Q}^{(s)} \end{bmatrix}}_{\Phi} X = \underbrace{\begin{bmatrix} Y \\ Y \\ Y \\ \vdots \\ Y \end{bmatrix}}_{\mathcal{Y}}. \tag{21}
$$

In general, there are more equations than unknowns in (21). Therefore, the equations are inconsistent and no solution exists. This implies that it is not possible to eliminate the harmonics at all velocities. Yet, in general, we can find the solution using all equations, but weight some more heavily, to minimize the error in the least square sense. Suppose $\mathbf{W}^{1/2}$ is a nonsingular diagonal matrix. Multiply both sides in (21) by $\mathbf{W}^{1/2}$

$$
\mathbf{W}^{1/2} \Phi X = \mathbf{W}^{1/2} \mathcal{Y}.
$$

Again the pseudo-inverse [3] offers a solution $X_{opt} = \left((\Phi^T \mathbf{W} \Phi)^{-1} \Phi^T \mathbf{W}^{1/2}\right) \mathcal{Y}$ with minimizes the following defined norm $\|\epsilon\|_W = \epsilon^T W \epsilon$, where

$$
\epsilon = \sum_{i=0}^{z} (Y - \mathbf{Q}^{(i)} X).
$$

Nevertheless, singular value decomposition is another technique (16) which can be applied here. In the following we will interpret the minimization criteria. Since $Q^{(i)}X = Y^{(i)}$ is a vector containing the real and imaginary part of the ripple spectrum at ith velocity, by proper choice of matrix $\mathbf{W}^{1/2}$ we can say

$$\|\epsilon\|_w^2 = \sum_{i=0}^{z} \left(w \left(\Delta^{(i)}\right)^2 + \sum_{j=1}^{2N/p} (\mathcal{R}e\ k_j^{(i)})^2 + (\mathcal{I}m\ k_j^{(i)})^2 \right), \tag{22}$$

where $\Delta^{(i)} = pk_0^{(i)} - 1$. By Parseval's equation we have

$$\|\tau^{(i)}\|_{rms} = \sum_{j=1}^{2N/p} |k_j^{(i)}|^2.$$

Therefore, the error function in (22) is equal to

$$\|\epsilon\|_w^2 = \sum_{i=0}^{s} \left(w(\Delta^{(i)})^2 + \sum_{i=0}^{s} \|\tau^{(i)}\|_{rms}^2 \right).$$

This means that the second commutation law minimizes the energy of the torque ripples and the weighted variation of torque transfer function.

4. Motor Characterization

Our simulation results in the following section are based on the parameters from the McGill/MIT direct drive motor [7], a synchronous motor with three phases and 18 poles. Both commutation laws require the knowledge of the torque-angle profile. If no torque sensor is available, the spectrum can be extracted by online identification based on back EMF measurements [1]. Alternatively, and this is the method used here, it can be characterized simply by torque measurements versus motor angle while one phase is energized with a constant current.

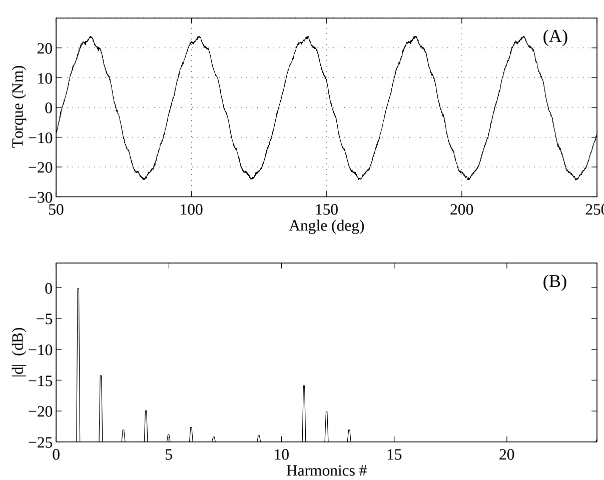

Figure 2: (A) Torque-angle profile of the motor. (B) The spectrum of $g(\theta)$.

The torque trajectory versus position was recorded during rotation, while one phase was energized with $12A$. For more precise results, the friction torque in motor bearing and rotor wire connections are subtracted from the torque trajectory. The resulting torque-angle profile and its harmonic content are shown in Fig. 2. The low frequency components in the spectrum are due to the distributed windings while the $12th$ is related to the number of slots (there are 108 slots and 9 pole pairs). The 11 and $13th$ harmonics are probably due to the multiplicative nature of interaction between the two sources of harmonics.

5. Simulation Results

We derived the commutation laws for the McGill/MIT motor, assuming a current amplifier with a bandwidth of $200Hz$. Using the theory developed in this paper, and the commutation spectra for minimum power losses and torque ripples were computed and are shown in Fig. 3. These simulations results show the tradeoffs clearly. If power losses are the main concern, a low bandwidth controller suffices, with only a few harmonic components. In order to minimize torque ripple as well, more energy dissipation resulted (19% more in our particular case), and the frequency component of the controller increased as well.

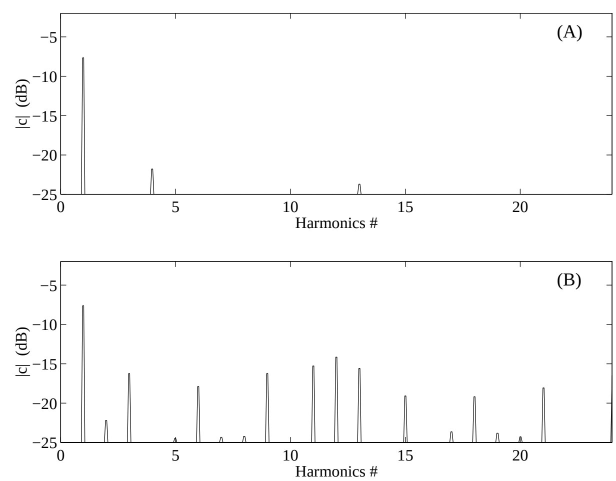

Figure 3: Commutation spectra for (A) minimal losses ($\|C\|_2 = 0.172$) and (B) minimal torque ripples ($\|C\|_2 = 0.188$).

In Fig. 4 the step response of the system when the first (A) and second (B) commutation laws are applied. The first one delivers smooth torque at very low speed (dashed line), but causes high ripple at high speed ($2rev/s$). The second one exhibits very low torque ripple at all velocities, even close to zero. However its losses are higher.

The frequency response of the linear counterpart of the torque system for both commutation laws is illustrated in the Fig. 4 C and D, respectively. The response of the system is coincident with that of the current amplifier at low velocities, but this is no longer valid as velocity rises.

This naturally increases the uncertainty of the system. A comparison in Fig. 4C,D clearly shows that the second commutation laws significantly introduces less uncertainty into the system. To show the impact of high velocity on the torque response, it is also calculated at $10 rev/s$ which is totally distorted from the current amplifier response.

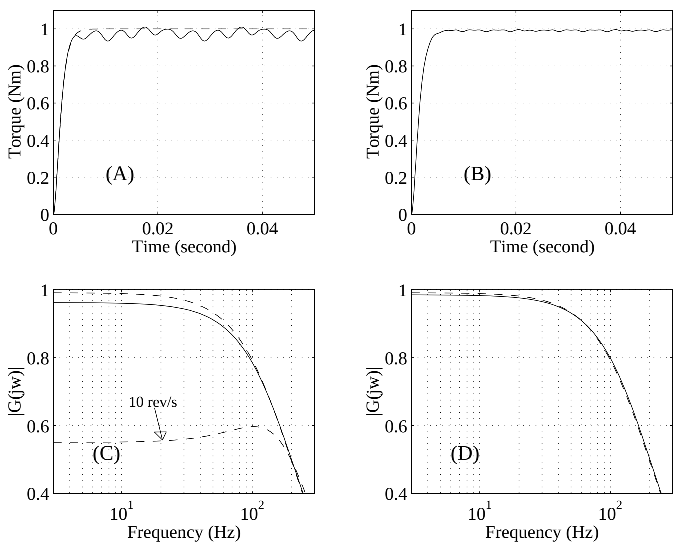

Figure 4: Step and frequency responses.

6. Conclusion

A general model for torque generation of synchronous motors in the presence of current amplifier dynamics is derived. The formulation uses Fourier coefficients to capture the phase torque and commutation function in a concise fashion. In addition, the calculation for commutation is simple and suitable for efficient implementation on DSP processors. We proposed two commutation laws. The first one minimizes copper losses, and can deliver a ripple-free torque independent of motor velocity, provided that the dynamics of the current amplifier are negligible. Otherwise, the motor velocity compromises performance in two ways. First, perfect ripple cancellation is not possible over a range of velocities. Moreover, the torque response of the system varies with velocity. We derived a commutation law addressing both issues. It minimizes the energy of the torque ripple and weighted uncertainty of torque transfer function due to motor velocity. Simulations using an experimentally derived torque characterization of a direct drive motor demonstrated the validity of this method.

Acknowledgements

This project was supported by the PRECARN TDS Project, through MPB Technologies of Montreal, Quebec.

References

[1] F. Aghili, M. Buehler, and J. M. Hollerbach. A new indirect adaptive control strategy for a synchronous direct drive motor. In *Proc. IEEE Int. Conf. Robotics and Automation*, pages 2865–2870, Minneapolis, MN, Apr 1996.

[2] C. H. An, C. G. Atkeson, and J. M. Hollerbach. *Model-Based Control of a Robot Manipulator*. MIT Press, Cambridge, MA, 1988.

[3] W. L. Brogan. *Modern Control Theory*. Prentice Hall, 1991.

[4] D. Chen and B. Paden. Adaptive linearization of hybrid step motors: stability analysis. *IEEE Trans. Automatic Control*, 38(6):874–887, June 1993.

[5] F. Filicori, C. G. Lo Bianco, and A. Tonielli. Modeling and control strategies for a variable reluctance direct-drive motor. *IEEE Trans. Industrial Electronics*, 40(1):105–115, 1993.

[6] R. M. Gray and J. W. Goodman. *Fourier Transforms*. Kluwer Academic Publishers, 1995.

[7] J. M. Hollerbach, I. Hunter, J. Lang, S. Umans, and R. Sepe. The McGill/MIT Direct Drive Motor Project. In *Proc. IEEE Int. Conf. Robotics and Automation*, pages 611–617, May 1993.

[8] P. C. Krause. *Analysis of electric machinery*. McGraw-Hill, 1986.

[9] D. G. Manzer, M. Varghese, and J. S. Thorp. Variable reluctance motor characterization. *IEEE Trans. Industrial Electronics*, 36(1):56–63, 1989.

[10] W. H. Press, B. P. Flannery, S. A. Teukolsy, and W. T. Vetterling. *Numerical Recipes in C*. Cambridge University Press, New York, 1988.

[11] D. G. Taylor. Nonlinear control of electric machines: An overview. *IEEE Control Systems*, 14(6):41–51, 1994.

[12] R. S. Wallace and D. G. Taylor. Low-torque-ripple switched reluctance motors for direct-drive robotics. *IEEE Trans. Robotics and Automation*, 7(6):733–742, 1991.